On the completeness of hierarchical tensor-product B-splines

Dominik Mokriš[a,*], Bert Jüttler[a], Carlotta Giannelli[a]

[a]*Institute of Applied Geometry, Johannes Kepler University of Linz, Altenberger Str. 69, 4040 Linz, Austria*

Abstract

Given a grid in $\mathbb{R}^d$, consisting of d bi-infinite sequences of hyperplanes (possibly with multiplicities) orthogonal to the d axes of the coordinate system, we consider the spaces of tensor-product spline functions of a given degree on a multi-cell domain. Such a domain consists of finite set of cells which are defined by the grid. A piecewise polynomial function belongs to the spline space if its polynomial pieces on adjacent cells have a contact according to the multiplicity of the hyperplanes in the grid. We prove that the connected components of the associated set of tensor-product B-splines, whose support intersects the multi-cell domain, form a basis of this spline space. More precisely, if the intersection of the support of a tensor-product B-spline with the multi-cell domain consists of several connected components, then each of these components contributes one basis function. In order to establish the connection to earlier results, we also present further details relating to the three-dimensional case with single knots only.

A hierarchical B-spline basis is defined by specifying nested hierarchies of spline spaces and multi-cell domains. We adapt the techniques from [12] to the more general setting and prove the completeness of this basis (in the sense that its span contains all piecewise polynomial functions on the hierarchical grid with the smoothness specified by the grid and the degrees) under certain assumptions on the domain hierarchy.

Finally, we introduce a decoupled version of the hierarchical spline basis that allows to relax the assumptions on the domain hierarchy. In certain situations, such as quadratic tensor-product splines, the decoupled basis provides the completeness property for any choice of the domain hierarchy.

Keywords: Hierarchical bases, Tensor-product B-splines, Local refinement, Decoupled hierarchical bases
2010 MSC: 65D07

1. Introduction

Hierarchical tensor-product splines were introduced by Forsey and Bartels [11] as a tool for adaptive surface modeling. About ten years later, Kraft [18] defined a basis and a quasi-interpolation operator for these spline spaces. At the same time, these splines were used for adaptive surface fitting [15].

Since the advent of isogeometric analysis (IGA), which was established in 2005 as a new approach to bridge the gap between analysis and design in engineering applications [6], there is a renewed interest in adaptive and hierarchical techniques for tensor-product splines.

*Corresponding author. Tel. +43(0)732 2468 4080
Email addresses: dominik.mokris@jku.at (Dominik Mokriš), bert.juettler@jku.at (Bert Jüttler), carlotta.giannelli@jku.at (Carlotta Giannelli)

The early approaches to adaptive refinement in IGA were based mostly on T-splines [1, 10]. These originated more recently than hierarchical B-splines in geometric modeling [28]. It was observed, however, that hierarchical B-splines possess a number of useful theoretical and practical properties that make them well-suited for numerical simulation based on IGA [29]. It has been shown that

- these adaptive splines can be equipped with a simple basis that provides the partition of unity and improves the sparsity properties [13];
- this basis is strongly stable with respect to the L_∞ norm [14];
- and these functions can be implemented efficiently using standard data structures [16].

There is a growing number of papers on hierarchical methods in IGA [5, 19, 26].

A new kind of splines has been introduced recently [9], known as LR-splines (LR stands for "locally refined"). The use of this new approach in the application context, as well as its comparison with existing local refinement methods, are still at a preliminary stage.

Simultaneously, adaptive and locally refined spline spaces were considered from an algebraic viewpoint. The general goal is to determine the dimension of the spline space (which contains all piecewise polynomial functions of a certain degree and smoothness) and to construct its basis, given a certain partition of the domain into axis-aligned boxes. In the rich literature on this topic [7, 8, 20, 21, 22, 23, 24, 27] several valuable contributions for various cases have been described.

Under certain conditions, the hierarchical spline basis spans the entire space of all piecewise polynomial functions of the given degree and smoothness that are defined on the underlying grid (which may possess T-joints) and is therefore *complete*. Such conditions were first studied in [12] for the bivariate case of uniform degrees, dyadic refinement and maximal smoothness. Based on the algebraic framework (homology techniques) described in [23], a number of recent manuscripts and preprints presented several generalizations. We mention the recent article [2] that addresses the three-dimensional case and the follow-up papers [4, 3].

The present paper introduces a different approach. It is based on the observation that the completeness of the hierarchical spline space can be studied without using advanced results from algebraic homology, but employing solely standard methods from the theory of tensor-product spline functions. The simple approach presented in this paper allows sufficient conditions to be derived for complete hierarchical spline spaces in any dimension, and for any smoothness (which does not have to be the same for all grid hyperplanes) and any degree.

The remainder of this paper consists of three main sections and an appendix. First we analyze dimensions and bases of tensor-product spline spaces on multi-cell domains in Section 2. The third section is devoted to the completeness of the hierarchical B-spline basis in the most general case. Finally, in Section 4 we introduce the decoupled hierarchical basis that allows to relax — and in some situations even to eliminate — the constraints on the considered domain hierarchy. The appendix analyzes the dimensions of tensor-product spline spaces in the trivariate case with single knots.

2. Splines on multi-cell domains

This section derives a basis for tensor-product splines on multi-cell domains. After presenting the necessary definitions, we will prove that this spline space is spanned by a basis consisting of all connected components of the tensor-product B-splines whose support intersects the multi-cell domain. More precisely, if the intersection of the support of a tensor-product B-spline with the multi-cell domain consists of several connected components, then each of them contributes one basis function.

2.1. Tensor-product B-splines

Given a positive integer d that specifies the dimension of the space, we consider the d–dimensional space $\mathbb{R}^d$ with coordinates $\mathbf{x} = (x_1, \ldots, x_d)$. In addition, we consider d bi-infinite strictly increasing sequences of real numbers

$$(g_{i,j})_{j\in\mathbb{Z}}, \quad g_{i,j} < g_{i,j+1},$$

for $i = 1, \ldots, d$, which will be called the *nodes*. Using these sequences of nodes we define the *grid* $\mathcal{G}$ to consist of *grid hyperplanes*

$$G_{i,j} = \{\mathbf{x} \in \mathbb{R}^d \mid x_i = g_{i,j}\}$$

with associated *multiplicities* $m_{i,j}$, which do not need to be the same for all the hyperplanes in the grid.

In addition, we choose a *degree* $\mathbf{p} = (p_1, \ldots, p_d)$, where all p_i are positive integers. We denote the set of tensor-product B-splines defined on this grid by B. More precisely, these tensor-product B-splines are products of d univariate B-splines with the variables x_i that are defined by the bi-infinite *knot vectors*

$$(\ldots, \underbrace{g_{i,j-1}, \ldots, g_{i,j-1}}_{m_{i,j-1}\text{ times}}, \underbrace{g_{i,j}, \ldots, g_{i,j}}_{m_{i,j}\text{ times}}, \underbrace{g_{i,j+1}, \ldots, g_{i,j+1}}_{m_{i,j+1}\text{ times}}, \ldots),$$

where each knot appears as often as specified by the multiplicity of the associated hyperplane. These tensor-product B-splines are well-defined and continuous if the multiplicities satisfy

$$1 \le m_{i,j} \le p_i. \tag{2.1}$$

In the sequel we will denote the tensor-product B-splines $\beta \in B$ simply as *B-splines*.

We consider d indices $j_1, \ldots, j_d \in \mathbb{Z}$. The closed set

$$\bigtimes_{i=1}^{d} [g_{i,j_i-1}, g_{i,j_i}], \tag{2.2}$$

which is the Cartesian product of d closed intervals between adjacent nodes, is called a *cell* of the grid. The *set of all cells* will be denoted by C and we use $c \in C$ to denote an individual cell.

Consider a cell $c \in C$. We define the set of all B-splines whose support includes this cell,

$$B_c = \{\beta \in B \mid c \subset \overline{\text{supp } \beta}\}, \tag{2.3}$$

where the symbol supp denotes the support of a function, i.e.,

$$\text{supp } g = \{\mathbf{x} \in \mathbb{R}^d \mid g(\mathbf{x}) \neq 0\}.$$

In the case of B-splines, this is an *open* set, provided that the multiplicity of each knot is at most equal to the degree as assumed in (2.1).

Example 2.1. Figure 1 shows an example of a set B_c. We consider biquadratic B-splines on a uniform grid with all multiplicities equal to 1. The cell c is shown in gray. The support of each basis function consists of 3×3 cells; the basis functions that belong to the set B_c are represented by the small circles in the centers of their supports, which coincide with their Greville points.

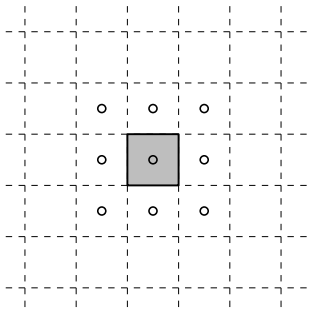

Figure 1: The set B_c for biquadratic B-splines with single knots. The small circles correspond to Greville points representing the functions in B_c with respect to the gray cell c.

Consider a *polynomial f of multi-degree* $\mathbf{p}$, i.e., f is a polynomial with the variables x_i, where the degree with respect to x_i is at most p_i. We denote the linear space of all such polynomials by $\Pi^{\mathbf{p}}(\mathbb{R}^d)$.

When restricting f and $\Pi^{\mathbf{p}}(\mathbb{R}^d)$ to this cell, we obtain the linear space

$$\Pi^{\mathbf{p}}(c) := \left\{ f|_c \mid f \in \Pi^{\mathbf{p}}(\mathbb{R}^d) \right\}.$$

The restriction $f|_c$ can be expressed as a linear combination of the tensor-product B-splines in B_c,

$$f|_c(\mathbf{x}) = \sum_{\beta \in B_c} \lambda_c^\beta(f|_c)\beta|_c(\mathbf{x}), \quad \mathbf{x} \in c, \tag{2.4}$$

where $\lambda_c^\beta(f|_c)$ is the coefficient of $\beta \in B_c$ in the local representation of the polynomial f on the cell c. Note that f is a polynomial defined on $\mathbb{R}^d$, whereas $f|_c$ is defined on c only.

Example 2.2. Consider again the example of biquadratic splines in Figure 1. Each cell $c \in C$ is influenced by nine basis functions from B_c and each biquadratic polynomial on this cell can be uniquely represented as a linear combination of these nine functions.

2.2. Contact of polynomial pieces

We denote the partial derivatives of a polynomial f by

$$\partial_i^j f := \frac{\partial^j f}{\partial (x_i)^j}.$$

Given a polynomial $f|_c$ on a cell c, we define its partial derivatives by considering its canonical extension to $\mathbb{R}^d$,

$$\partial_i^j(f|_c) := (\partial_i^j f)|_c,$$

thereby avoiding the need to consider one-sided limits at the boundary of c.

Consider two cells $c, c' \in C$. There exist indices $j_i, j_i' \in \mathbb{Z}$ such that

$$c = \bigtimes_{i=1}^{d} [g_{i,j_i}, g_{i,j_i+1}] \quad \text{and} \quad c' = \bigtimes_{i=1}^{d} [g_{i,j_i'}, g_{i,j_i'+1}].$$

The intersection of these cells is an axis-aligned box whose dimension is at most d. If the intersection is non-empty, then it can be written as

$$c \cap c' = \bigtimes_{i=1}^{d} [g_{i,a_i}, g_{i,b_i}], \tag{2.5}$$

where $a_i = \max\{j_i, j_i'\}$ and $b_i = \min\{j_i, j_i'\} + 1$. Note that the i–th interval (where $i = 1, \ldots, d$) in the Cartesian product degenerates to a single point if $j_i = j_i' + 1$ or $j_i' = j_i + 1$.

Definition 2.3. Consider two polynomials f, f' of degree $\mathbf{p}$ and two cells $c, c' \in C$, thus $f|_c \in \Pi^{\mathbf{p}}(c)$ and $f'|_{c'} \in \Pi^{\mathbf{p}}(c')$. We say that the polynomial $f|_c$ on the cell c and the polynomial $f'|_{c'}$ on the cell c' have a *contact* on $c \cap c'$ (and write $f|_c \sim f'|_{c'}$) if

$$\forall \mathbf{x} \in c \cap c' : \ (\partial_1^{j_1} \cdots \partial_d^{j_d} f|_c)(\mathbf{x}) = (\partial_1^{j_1} \cdots \partial_d^{j_d} f'|_{c'})(\mathbf{x}) \tag{2.6}$$

is satisfied for all

$$j_i = 0, \ldots, p_i - \min\{m_{i,a_i}, m_{i,b_i}\}, \quad i = 1, \ldots, d, \tag{2.7}$$

where $c \cap c'$ has the form (2.5) (or is empty) and m_{i,a_i} and m_{i,b_i} are the multiplicities of the grid hyperplanes G_{i,a_i} and G_{i,b_i}, respectively.

In particular, any two polynomials on disjoint cells have a contact, since $c \cap c'$ is empty in this case. The relation $\sim$, which acts on pairs of polynomials and cells, is symmetric and reflexive, but not transitive.

The order of the contact depends on the given multiplicity of the grid hyperplanes: the higher the multiplicity, the smaller the number of derivatives that have to agree.

Note that if $a_i < b_i$ holds for some coordinate direction i in the representation (2.5) of the (nonempty) intersection $c \cap c'$ (namely, when $j_i = j_i'$), then the equation (2.6) is even satisfied for *all* positive integers j_i, since we can differentiate the equations obtained for the ranges of indices j_i specified in (2.7) with respect to x_i.

From now on we will use the notation

$$\beta|_{c \cap c'} \neq 0$$

to express the fact that the B-spline β does not vanish identically on $c \cap c'$, i.e.,

$$\exists \mathbf{x} \in c \cap c' : \beta(\mathbf{x}) \neq 0.$$

The contact between two polynomials on different cells can be characterized easily with the help of the B-spline coefficients.

Lemma 2.4 (Contact Characterisation Lemma – CCL)**.** *The two polynomials $f|_c$ and $f'|_{c'}$ that were considered in Definition 2.3 have a contact on $c \cap c'$ if and only if*

$$\forall \beta : \beta|_{c \cap c'} \neq 0 \Rightarrow \lambda_c^{\beta}(f|_c) = \lambda_{c'}^{\beta}(f'|_{c'}). \tag{2.8}$$

Proof. This can be proved by extending the univariate blossoming argument to the tensor-product setting (see, e.g., [25, Section 7.1]; the extension would proceed analogously to the similar generalization for multivariate Bézier surfaces, which is outlined in [25, Section 9.7]). Indeed, the two polynomials have a contact if and only if the associated values of their blossoms (which then correspond to the B-spline coefficients) agree.

Alternatively, one may prove this observation with the help of the tensor-product Bernstein-Bézier (BB) representation of the two polynomials with respect to the associated cells. The

values and derivatives that characterize the contact are uniquely determined by the two subsets of the BB coefficients (determining sets) of both polynomials. The polynomials have a contact if and only if the coefficients of the determining set of $f|_c$ can be generated by applying a certain bijective linear mapping to the coefficients of the determining set of $f'|_{c'}$. On the other hand, the subset of the B-spline coefficients considered in (2.8) is linked to each of the coefficients of the two determining sets by two other bijective linear mappings that can be found via knot insertion. Due to the bijectivity of all mappings, choosing the same B-spline coefficients considered in (2.8) for both polynomials is the only possibility to obtain a contact.

In order to keep this paper concise, we do not present the technical details of either proof. □

Example 2.5. We consider the bivariate case with double horizontal knots and single vertical knots in Figure 2. There are sixteen bicubic B-splines whose supports intersect each cell (a). Considering two cells that are different from each other, there are four possibilities of a contact between polynomials.

- The cells are disjoint and all polynomials have a contact (not shown).
- The cell share a vertical edge (b). All values and derivatives of order 0 or 1 with respect to x_1 and of any order with respect to x_2 have the same value on the vertical edge.
- The cells share a horizontal edge (c). All values and derivatives of any order with respect to x_1 and of order 0, 1, or 2 with respect to x_2 have the same value on the horizontal edge.
- The cells share a grid point (d). All values and derivatives of order 0 and 1 with respect to x_1 and of order 0, 1, or 2 with respect to x_2 have the same value at the grid point.

2.3. Piecewise polynomials on multi-cell domains

We consider a finite subset $M \subset C$ which we will call a *multi-cell domain*. More precisely, the set M contains a finite number of cells of the form (2.2). Furthermore, we will use the abbreviation

$$\mathcal{M} = \bigcup M = \bigcup_{c \in M} c$$

for the subset of $\mathbb{R}^d$ occupied by the cells from M. The set $\mathcal{M}$ is a closed and bounded subset of $\mathbb{R}^d$. To simplify the notation it will be often also called multi-cell domain, whenever confusion is improbable.

Definition 2.6. Given a multi-cell domain $M \subset C$ we define the *disconnected space* (also called *the space of piecewise polynomials*) by

$$\mathbb{P}(M) = \{s = (s_c)_{c \in M} \mid s_c \in \Pi^{\mathbf{p}}(c)\}.$$

Thus any piecewise polynomial $s \in \mathbb{P}(M)$ is a collection of polynomials s_c, one for each cell $c \in M$. Each of these polynomials s_c is actually the restriction of a globally defined polynomial $\bar{s}_c \in \Pi^{\mathbf{p}}(\mathbb{R}^d)$ to the corresponding cell, i.e., $s_c = \bar{s}_c|_c$ — see the end of Subsection 2.1. However, we will not need to refer to the globally defined polynomials $\bar{s}_c$ throughout the paper.

Note that these polynomials may take different values at the grid lines. Therefore, it is generally impossible to define a continuous function $\hat{s}$ on $\mathcal{M}$ such that $\hat{s}|_c = s_c$ for all $c \in M$.

Nevertheless, each s_c can be represented in the B-spline basis as observed in (2.4):

$$s_c(\mathbf{x}) = \sum_{\beta \in B_c} \lambda_c^\beta(s_c)\beta|_c(\mathbf{x}), \quad \mathbf{x} \in c, \quad c \in M.$$

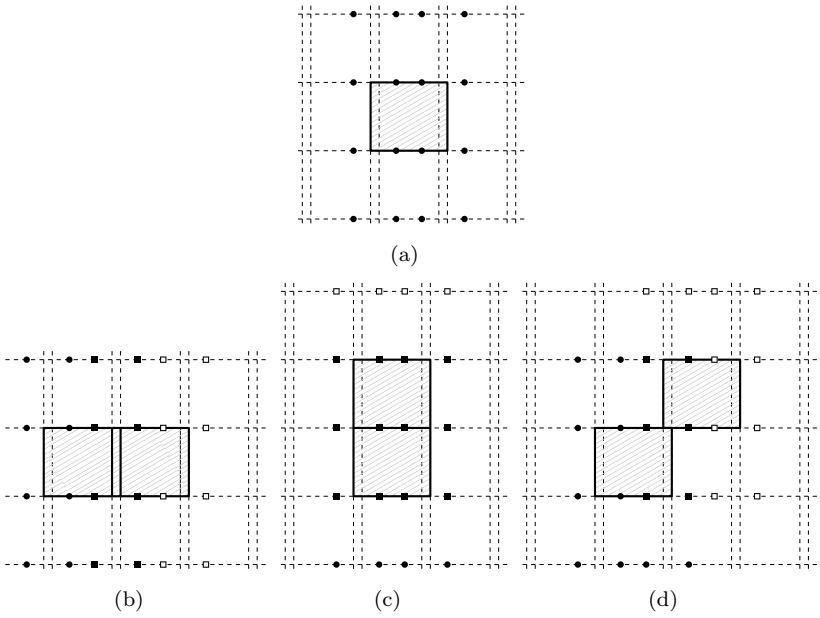

Figure 2: (a) The 16 bicubic B-splines in B_c related to the case of double horizontal and single vertical knots; (b) – (d) three possibilities of a contact. The B-splines whose supports intersect the first and second cell are depicted by solid symbols (●, ■) and by squares (■, □), respectively. The support of any B-spline represented by a solid square (■) intersects both cells.

Definition 2.7. We consider a multi-cell domain M and the associated disconnected space $\mathbb{P}(M)$. The *spline space* on M is defined by

$$\mathbb{S}(M) = \{s \in \mathbb{P}(M) \mid \forall c, c' \in M : s_c \sim s_{c'}\}. \tag{2.9}$$

For $s \in \mathbb{S}(M)$ we define $\tilde{s} : \mathcal{M} \to \mathbb{R}$ so that

$$\tilde{s}(\mathbf{x}) = s_c(\mathbf{x}), \quad \text{if } \mathbf{x} \in c \text{ and } c \in M.$$

This function is well-defined (single-valued), since any two polynomial pieces s_c and $s_{c'}$ meet at least continuously along the intersection $c \cap c'$ of any two neighbouring cells. By using the characteristic functions χ_c of the cells $c \in M$, we may express it in terms of the basis functions as follows:

$$\tilde{s}(\mathbf{x}) = \sum_{c \in M} \sum_{\beta \in B_c} \lambda_c^\beta(s_c)\beta(\mathbf{x})\chi_c^\star(\mathbf{x}), \quad \mathbf{x} \in \mathcal{M}, \tag{2.10}$$

with the normalized characteristic functions

$$\chi_c^\star(\mathbf{x}) = \begin{cases} \dfrac{\chi_c(\mathbf{x})}{\sum_{k \in M} \chi_k(\mathbf{x})}, & \text{if} \quad \mathbf{x} \in \mathcal{M}, \\ 0, \quad \text{otherwise.} \end{cases}$$

Note that the characteristic functions need to be normalized in order to obtain the correct values also on grid hyperplanes.

Strictly speaking, the elements of $\mathbb{S}(M)$ are $|M|$–tuples of polynomials, where $|M|$ is the number of cells in M. In order to keep the notation simple, we will use the same notation for the actual spline functions $\tilde{s}$.

That is, we will consider the elements of $\mathbb{S}(M)$ simultaneously as $|M|$–tuples of polynomials and as piecewise polynomial functions defined on $\mathcal{M}$. Consequently, we will simply write s instead of $\tilde{s}$, and we will denote the *linear space of all piecewise polynomial functions on $\mathcal{M}$ with the required contacts* between the polynomial segments as $\mathbb{S}(M)$.

Definition 2.8. Consider a basis function $\beta \in B$. Its *coefficient graph* Γ_β is defined as follows.

- The vertices of Γ_β are the cells $c \in M$ such that $c \subset \overline{\text{supp } \beta}$.
- Two vertices c and c' are connected by an edge iff $\beta|_{c \cap c'} \neq 0$.

The *set of connected components* of this graph will be denoted by $K(\Gamma_\beta)$.

If there is no overlap of β with $\mathcal{M}$ then both the coefficient graph Γ_β and the set $K(\Gamma_\beta)$ of connected components are empty.

We use the notation

$$c \,\varepsilon\, \Gamma_\beta$$

to express the fact that *the cell c is a vertex of the coefficient graph Γ_β*. Similarly, when considering a connected component $\Phi \in K(\Gamma_\beta)$ — which is a subgraph of Γ_β — all cells c satisfying $c \,\varepsilon\, \Phi$ are exactly the vertices of Φ.

Example 2.9. We consider again the biquadratic case. Figure 3 shows a multi-cell domain consisting of nine cells (a), the supports of three basis functions β_1, β_2 and β_3 (b), together with their coefficient graphs (c). The coefficient graphs of β_2 and β_3 have only one connected component, while the coefficient graph of β_1 possesses two of them.

Proposition 2.10. *Consider a piecewise polynomial $s \in \mathbb{P}(M)$. It is contained in the spline space $\mathbb{S}(M)$ if and only if the coefficients satisfy $\lambda_c^\beta(s_c) = \lambda_{c'}^\beta(s_{c'})$ for all basis functions $\beta \in B$ and for all c and c' belonging to the same connected component of Γ_β.*

Proof. Consider a piecewise polynomial $s \in \mathbb{S}(M)$ and a basis function $\beta \in B$. Assume there exist c, c' in the same connected component such that $\lambda_c^\beta(s_c) \neq \lambda_{c'}^\beta(s_{c'})$. Then there exist two vertices k and k', $k \cap k' \neq \emptyset$, in this connected component such that $\lambda_k^\beta(s_k) \neq \lambda_{k'}^\beta(s_{k'})$. According to CCL (Lemma 2.4), s_k and $s_{k'}$ do not have a contact and therefore s does not belong to $\mathbb{S}(M)$.

On the other hand, if all coefficients $\lambda_c^\beta(s_c)$ associated to any $\beta \in B$ for all cells c belonging to one connected component of Γ_β take the same value, then all s_c have a contact by CCL (Lemma 2.4). Since the cells in these connected components cover M, we may conclude that $s \in \mathbb{S}(M)$. □

2.4. Spline bases on multi-cell domains

Definition 2.11. For every $\beta \in B$ and every connected component $\Phi \in K(\Gamma_\beta)$ we define the function

$$\beta_\Phi(\mathbf{x}) = \sum_{c \,\varepsilon\, \Phi} \beta(\mathbf{x}) \chi_c^\star(\mathbf{x}).$$

The set of all these functions is denoted by

$$\Delta = \bigcup_{\beta \in B} \{\beta_\Phi \mid \Phi \in K(\Gamma_\beta)\}.$$

Theorem 2.12. *The set Δ — when restricted to $\mathcal{M}$ — forms a locally linearly independent basis of $\mathbb{S}(M)$.*

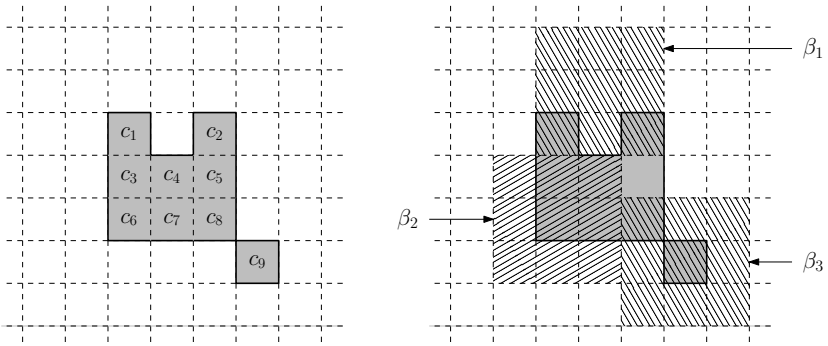

(a) multi-cell domain (b) three examples of B-splines β_i

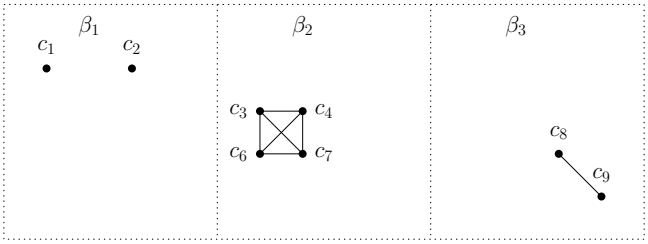

(c) coefficient graphs associated with β_i, $i = 1, 2, 3$

Figure 3: A multi-cell domain with nine cells (a), the supports of three biquadratic B-splines (b) and the associated coefficient graphs (c).

Proof. Consider $s \in \mathbb{S}(M)$. First, we prove that s can be obtained as a linear combination of functions from Δ. Since, according to Definition 2.8, the vertices of Γ_β are the cells $c \in M$ that are contained in the support of β, equation (2.10) can be rewritten as follows:

$$s(\mathbf{x}) = \sum_{\beta \in B} \sum_{c \,\varepsilon\, \Gamma_\beta} \lambda_c^\beta(s_c)\beta(\mathbf{x})\chi_c^\star(\mathbf{x}) = \sum_{\beta \in B} \sum_{\Phi \in K(\Gamma_\beta)} \sum_{c \,\varepsilon\, \Phi} \lambda_c^\beta(s_c)\beta(\mathbf{x})\chi_c^\star(\mathbf{x}), \tag{2.11}$$

where $\mathbf{x} \in \mathbb{R}^d$. In virtue of Proposition 2.10, for each $\beta \in B$ and for each $\Phi \in K(\Gamma_\beta)$, all the coefficients $\lambda_c^\beta(s_c)$ have to be the same for all $c \,\varepsilon\, \Phi$. We will denote this coefficient by $\Lambda_\Phi^\beta(s)$. Thus, we may rewrite (2.11) as

$$s(\mathbf{x}) = \sum_{\beta \in B} \sum_{\Phi \in K(\Gamma_\beta)} \Lambda_\Phi^\beta(s) \underbrace{\sum_{c \,\varepsilon\, \Phi} \beta(\mathbf{x})\chi_c^\star(\mathbf{x})}_{=\beta_\Phi \in \Delta}.$$

Second, we prove the local linear independence of the functions. Consider an open subset $X \subset \mathcal{M}$ and a linear combination of functions $\beta_\Phi \in \Delta$ that do not vanish on X, which is equal to zero on X. For each β_Φ we consider a cell $c \,\varepsilon\, \Phi$, that has a nonempty intersection with X. Clearly, β_Φ does not vanish on c. Moreover, the restrictions of all functions β_Φ to this cell are either zero or equal to the restrictions of mutually different tensor-product B-splines $\beta \in B$. From the local linear independence of functions $\beta \in B$ we then obtain that the coefficient of β_Φ in the linear combination is zero. Repeating this for all functions β_Φ, we conclude that the functions β_Φ are locally linearly independent. This also implies the linear independence of Δ. □

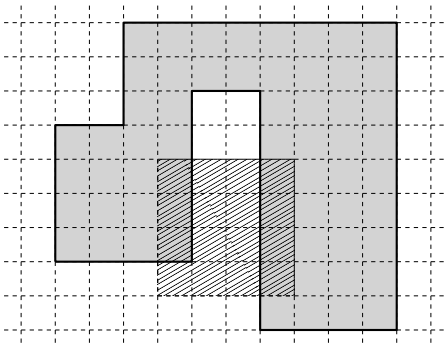

Figure 4: The support of a bicubic B-spline that violates the assumption of Corollary 2.13 with respect to the domain consisting of all the gray cells.

Corollary 2.13. *If for each β the intersection of its support with the multi-cell domain $\mathcal{M}$ is connected, then the functions in*

$$B_M = \{\beta \in B \mid \operatorname{supp} \beta \cap \mathcal{M} \neq \emptyset\},$$

when restricted to $\mathcal{M}$, form a basis of $\mathbb{S}(M)$.

Proof. Indeed, if this condition is satisfied, then each coefficient graph in Theorem 2.12 has either one connected component or it is empty. □

Example 2.14. The condition concerning the connected sets in Corollary 2.13 means that there is no situation like the one shown in Figure 4 for bicubic B-splines on a grid with single knots.

Appendix A analyzes the case of trivariate spline spaces with single knots, which has been discussed in Berdinsky et al. [2]. We show that their result (which, however, is limited to a special class of multi-cell domains) is a special case of Corollary 2.13.

3. Hierarchical splines

We now use the notation introduced in the previous section in a hierarchical setting to define a hierarchical spline space and a certain hierarchical basis. Subsequently, we prove that this hierarchical basis spans the entire hierarchical spline space.

3.1. Hierarchies of tensor-product spline spaces

In order to define a hierarchical tensor-product spline space, we need to introduce a hierarchy of tensor-product spline spaces and a hierarchy of domains.

First, we consider the spline spaces. Given a maximal level N, we consider a sequence of grids $\mathcal{G}^\ell$, $\ell = 0, \dots, N$, with associated degrees $\mathbf{p}^\ell = (p_1^\ell, \dots, p_d^\ell)$ where we assume that the *degrees do not decrease*,

$$\mathbf{p}^\ell \leq \mathbf{p}^{\ell+1}, \quad \text{that is} \quad p_i^\ell \leq p_i^{\ell+1}, \qquad i = 0, \dots, d, \quad \ell = 0, \dots, N-1.$$

Each grid hyperplane $G_{i,j}^\ell \in \mathcal{G}^\ell$ has an associated multiplicity $m_{i,j}^\ell$ that satisfies the assumption (2.1) level by level.

We assume that the *grids are nested* in the following sense: every grid hyperplane in $\mathcal{G}^\ell$ is also present in $\mathcal{G}^{\ell+1}$ and its multiplicity in the higher level is at least equal to the previous multiplicity plus the increase of the degree in the corresponding coordinate direction.

Based on the sequence of grids and degrees, we now define on each grid $\mathcal{G}^\ell$ the set of tensor-product B-splines B^ℓ of degree $\mathbf{p}^\ell$. The spans of the B-splines define the spline spaces

$$\mathbb{V}^\ell = \operatorname{span} B^\ell, \quad \ell = 0, \dots, N.$$

Under the previous assumptions concerning non-decreasing degrees and nested grids, the linear spaces spanned by the B-splines are nested, i.e.,

$$\mathbb{V}^\ell \subseteq \mathbb{V}^{\ell+1}, \quad \ell = 0, \dots, N-1.$$

For each level ℓ, the grid $\mathcal{G}^\ell$ and the degrees $\mathbf{p}^\ell$ allow to apply the theory from Section 2. Thus, if we are given a multi-cell domain M^ℓ with respect to the grid $\mathcal{G}^\ell$, we may define a spline space $\mathbb{S}^\ell(M^\ell)$. Note that the restriction of $\mathbb{V}^\ell$ to $\mathcal{M}^\ell$ is contained in this spline space,

$$\mathbb{V}^\ell|_{\mathcal{M}^\ell} \subseteq \mathbb{S}^\ell(M^\ell).$$

The connected components of the B-splines from B^ℓ with respect to the multi-cell domain

$$\mathcal{M}^\ell = \bigcup_{c \in M^\ell} c$$

form a basis of this space according to Theorem 2.12.

In addition, we consider a *nested sequence of domains*

$$\Omega^0 \supseteq \Omega^1 \supseteq \cdots \supseteq \Omega^N = \emptyset, \tag{3.1}$$

which will be called the *domain hierarchy*. We assume that these domains satisfy the following.

Assumption 3.1. *Each set*

$$\Omega^0 \setminus \Omega^{\ell+1}, \quad \ell = 0 \dots N-1,$$

can be represented as a multi-cell domain with respect to the grid $\mathcal{G}^\ell$. More precisely, we assume that there exists a multi-cell domain $M^\ell \subseteq C^\ell$, which is a finite set of cells of the grid $\mathcal{G}^\ell$, satisfying

$$\Omega^0 \setminus \Omega^{\ell+1} = \mathcal{M}^\ell.$$

For convenience, we define

$$\mathcal{M}^{-1} = \emptyset.$$

The sets

$$\mathcal{M}^\ell = \Omega^0 \setminus \Omega^{\ell+1}$$

were denoted as *rings* in [12], because, conceptually, they represent the domain Ω^0 with the "hole" $\Omega^{\ell+1}$. We will also adopt this concept. However, the above assumption concerning the shape of the rings is actually weaker than the one in [12], where each Ω^ℓ was assumed to be a multi-cell domain of level $\max(0, \ell - 1)$.

Note that these rings are also nested,

$$\Omega^0 = \mathcal{M}^{N-1} \supseteq \mathcal{M}^{N-2} \supseteq \cdots \supseteq \mathcal{M}^0 \supseteq \mathcal{M}^{-1} = \emptyset.$$

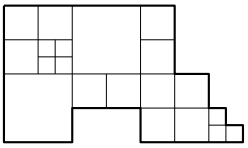

Figure 5: Hierarchical mesh consisting of cells from three levels.

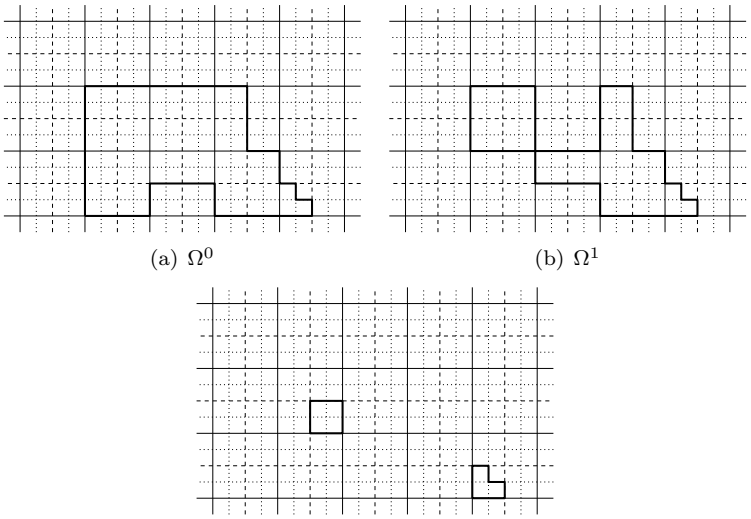

(a) Ω^0 (b) Ω^1

(c) Ω^2

Figure 6: Domains Ω^0, Ω^1 and Ω^2 associated with the mesh in Figure 5. Grid lines from level $0, 1, 2$ are depicted as solid, dashed, and dotted lines, respectively

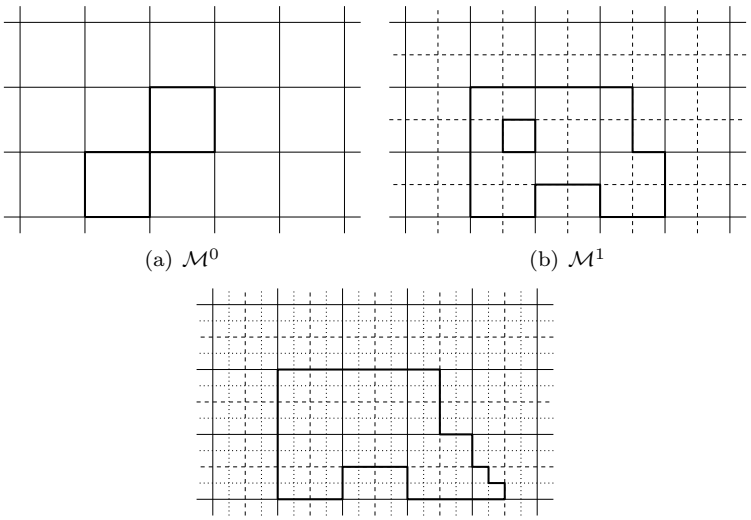

(a) $\mathcal{M}^0$ (b) $\mathcal{M}^1$

(c) $\mathcal{M}^2$

Figure 7: Rings associated with the mesh in Figure 5.

Example 3.2. Figure 5 shows a hierarchical mesh. The corresponding domains are shown in Figure 6 and the associated rings are depicted in Figure 7. As already mentioned, Assumption 3.1 does not require the boundary of each Ω^ℓ to be aligned with the knots lines associated to the previous level $\ell - 1$, as it was assumed in [12]. For instance, the small L-shaped subdomain at level 2 on the bottom right corner of the mesh was disallowed in [12].

Based on the sequences of function spaces and domains, we are now able to define the hierarchical spline space, provided that the restriction of a function to each of the multi-cell domains $\mathcal{M}^\ell$ belongs to the corresponding spline space $\mathbb{S}^\ell(M^\ell)$:

Definition 3.3. The *hierarchical spline space* $\mathbb{H}$ is given by

$$\mathbb{H} = \{h : \Omega^0 \to \mathbb{R} \mid \forall \ell : h|_{\mathcal{M}^\ell} \in \mathbb{S}^\ell(M^\ell)\}.$$

According to this definition, a function is contained in the hierarchical space if it is a piecewise polynomial function on the hierarchical grid defined by the nested grids and domains, where the individual polynomial segments meet with the smoothness specified by the degrees and the multiplicities of the grid hyperplanes. Note that this is more general than just requiring that

$$h|_{\mathcal{M}^\ell} \in \mathbb{V}^\ell|_{\mathcal{M}^\ell}.$$

3.2. The basis of the hierarchical spline space

Recall that we have defined a tensor-product spline basis B^ℓ on each grid $\mathcal{G}^\ell$. Similarly to (2.3) we consider the B-splines whose support intersects the ring $\mathcal{M}^\ell$:

$$B^\ell_{M^\ell} := \{\beta \in B^\ell \mid \operatorname{supp} \beta \cap \mathcal{M}^\ell \neq \emptyset\}.$$

Based on the definition of the rings, we again use the selection procedure from [12], which slightly generalizes the earlier method proposed by Kraft in [18] by also allowing for coinciding subdomain boundaries.

Definition 3.4. The *hierarchical basis* $\mathcal{K}$ is defined as

$$\mathcal{K} = \bigcup_{\ell=0}^{N-1} \mathcal{K}^\ell$$

with

$$\mathcal{K}^\ell = \{\beta \in B^\ell_{M^\ell} \mid \operatorname{supp} \beta \cap \mathcal{M}^{\ell-1} = \emptyset\}.$$

Thanks to the local linear independence of the bases $\mathcal{K}^\ell \subset B^\ell$, it can be shown that the set $\mathcal{K}$ of hierarchical B-splines is linearly independent, see [18] or [29].

Now we are able to formulate the main result of this paper.

Theorem 3.5. *If the assumption of Corollary 2.13 is satisfied for each level ℓ, i.e., if for any $\ell = 0, \dots, N-1$, and any $\beta \in B^\ell$ the set* $\operatorname{supp} \beta \cap \mathcal{M}^\ell$ *is connected, then the hierarchical spline basis $\mathcal{K}$ from Definition 3.4 spans the entire space $\mathbb{H}$.*

Proof. The proof is rather similar to the proof of Theorem 20 in [12]. Nevertheless, in order to make this paper self-contained, we repeat it here in a shorter form.

We consider a function $h \in \mathbb{H}$. The proof consists of two steps. First, we show that there exist N functions $h^\ell \in \operatorname{span} B^\ell_{M^\ell}$, $\ell = 0, \dots, N-1$, such that

$$h^\ell|_{\mathcal{M}^\ell} = \left(h - \sum_{i=0}^{\ell-1} h^i \right) \Big|_{\mathcal{M}^\ell}. \tag{3.2}$$

This can be proved by induction with respect to ℓ. In each step, the right hand side of (3.2) can be shown to belong to $\mathbb{S}^\ell(M^\ell)$, hence Corollary 2.13 implies the existence of h^ℓ.

Second, it can be shown by analyzing the right-hand side of equation (3.2) that $h^\ell|_{\mathcal{M}^{\ell-1}} = 0$. Therefore, the local linear independence of the B-splines implies that $h^\ell \in \operatorname{span} \mathcal{K}^\ell$.

Finally, by rewriting (3.2) for $\ell = N-1$, we obtain

$$h|_{\mathcal{M}^{N-1}} = \sum_{i=0}^{N-1} h^i|_{\mathcal{M}^{N-1}},$$

which concludes the proof, since $\mathcal{M}^{N-1} = \Omega^0$, $h^i \in \operatorname{span} \mathcal{K}^i$, and $\bigcup_{i=0}^{N-1} \mathcal{K}^i = \mathcal{K}$. □

The assumptions of Theorem 3.5 are satisfied if each subdomain Ω^ℓ is either sufficiently small or sufficiently large with respect to the supports of the B-splines at the previous level. This condition is slightly weaker than the assumptions of Theorem 20 in [12].

Example 3.6. Consider the case where all the degrees (at all levels and in all coordinate directions) are equal to p and all the multiplicities of hyperplanes are equal to 1. In this case, when considering dyadic refinement only, a sufficient condition for the assumptions of Theorem 3.5 to be satisfied is that there is a finite set I such that

$$\Omega^\ell = \bigcup_{i \in I} \Omega_i^\ell, \text{ where } \left(\Omega_i^\ell\right)^\circ \cap \left(\Omega_j^\ell\right)^\circ = \emptyset \quad \text{for } i, j \in I,\ i \neq j$$

(that is, the interiors of the sets Ω_i^ℓ are mutually disjoint) and each Ω_i^ℓ is such that either

- $\Omega^0 \setminus \Omega_i^\ell$ admits an *offset*[1] at distance $(p-1)/2$ with respect to the grid $\mathcal{G}^{\ell-1}$ or
- Ω_i^ℓ is contained in a box consisting of $(p-1) \times \cdots \times (p-1)$ cells of the grid $\mathcal{G}^{\ell-1}$.

Figure 8 provides a bivariate example.

4. The decoupled hierarchical basis

We introduce a *decoupling* mechanism, which is inspired by the so-called *truncation* introduced in [13]. It can be suitably exploited in order to relax the assumptions of Theorem 3.5.

We consider the representation of a B-spline β with respect to the next (i.e., finer) level in the spline hierarchy. For each connected component of β we define a decoupled basis function. This function collects the contributions of those functions of the next level whose supports have an overlap with a particular connected component of the support of the original B-spline β, restricted to the associated multi-cell domain $\mathcal{M}^\ell$.

More precisely, we consider the representation of a B-spline $\beta \in B^\ell$ with respect to the basis $B^{\ell+1}$ at the next level given by

$$\beta = \sum_{\gamma \in B^{\ell+1}} c_\gamma^{\ell+1}(\beta)\gamma,$$

with certain coefficients $c_\gamma^{\ell+1}(\beta) \in \mathbb{R}$, which are determined by the knot insertion algorithm. The function β possesses an associated coefficient graph Γ_β^ℓ with respect to the multi-cell domain M^ℓ, see Definition 2.8. We consider the connected components $K(\Gamma_\beta^\ell)$ of the coefficient graph and use each of them to define a decoupled function.

[1]The *offset* to a domain and its admissibility have been defined in [12] for the case $d = 2$ and they are defined in Appendix A for $d = 3$. The latter definition extends to any dimension d.

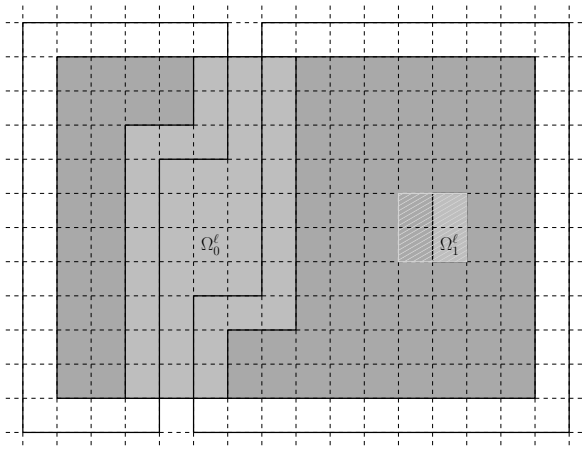

Figure 8: A domain $\Omega^\ell = \Omega_0^\ell \cap \Omega_1^\ell$ that satisfies the assumptions of Theorem 3.5 for $p = 3$ as specified in Example 3.6. We show the interior of $\Omega^0 \setminus \Omega^\ell$ (dark gray cells), Ω_0^ℓ and Ω_1^ℓ (light gray cells), the offset of $\Omega^0 \setminus \Omega_0^\ell$ at distance 1 (thick black line) and a box of 2×2 cells containing Ω_1^ℓ (hatched light gray cells). The dashed lines represent the grid $\mathcal{G}^{\ell-1}$.

Definition 4.1. For each connected component $\Phi \in K(\Gamma_\beta^\ell)$ we define a *decoupled basis function*

$$\delta_\Phi(\beta) = \sum_{\gamma \in B^{\ell+1}:\ \text{supp}\ \gamma \cap (\bigcup \Phi) \neq \emptyset} c_\gamma^{\ell+1}(\beta)\gamma, \quad \Phi \in K(\Gamma_\beta^\ell),$$

where $\bigcup \Phi = \bigcup_{c \in \Phi} c$ denotes the union of the cells that are vertices of Φ. If the support of each function $\gamma \in B^{\ell+1}$ intersects at most one of the sets $\bigcup \Phi$, then so do the functions $\delta_\Phi(\beta)$. We say that the decoupling is *feasible* if this condition is satisfied for all $\beta \in B^\ell$ and for all levels ℓ.

If the decoupling is feasible, then the restriction of the decoupled basis function $\delta_\Phi(\beta)$ to the multi-cell domain $\mathcal{M}^\ell$ is identical to the function β_Φ that was defined in Definition 2.11. Consequently, the decoupled functions inherit the properties of these functions. In particular, Theorem 2.12 implies the following result.

Corollary 4.2. *If the decoupling is feasible, then the functions from the set*

$$D_{M^\ell}^\ell := \{\delta_\Phi(\beta) \,|\, \Phi \in K(\Gamma_\beta^\ell),\ \beta \in B_{M^\ell}^\ell\}, \tag{4.1}$$

when restricted to $\mathcal{M}^\ell$, form a locally linearly independent basis of $\mathbb{S}^\ell(M^\ell)$.

Generally, the feasibility of the decoupling depends on the choice of the domains Ω^ℓ, $\ell = 0, \dots, N$. For certain classes of spline spaces $\mathbb{V}^\ell, \ell = 0, \dots, N-1$, however, the decoupling is always feasible. We introduce the following definition.

Definition 4.3. A sequence of nested spline spaces $(\mathbb{V}^\ell)_{\ell=0}^{N-1}$ is said to possess the *unconstrained completeness property (UCP)* if the decoupling is feasible at all levels and for any choice of the domains Ω^ℓ.

UCP is automatically granted if the support of each function of level $\ell + 1$ is contained in $2 \times 2 \times \cdots \times 2$ cells of the grid of level ℓ. Indeed, if this condition is satisfied, then for any choice of the multi-cell domain M^ℓ, the intersection of the support of a finer function with this multi-cell domain is connected. Special instances of this situation will be presented in Examples 4.5 and 4.6 below.

Corollary 4.4. *The functions contained in*

$$D = \bigcup_{\ell=0}^{N-1} \{\delta_\Phi(\beta) \in D^\ell_{M^\ell} \,|\, \text{supp } \delta_\Phi(\beta) \cap \mathcal{M}^{\ell-1} = \emptyset\} \tag{4.2}$$

form a basis of the space $\mathbb{H}$, which was introduced in Definition 3.3, provided that the decoupling is feasible at all levels. In particular, if the sequence of nested spline spaces has the unconstrained completeness property, then this is true for any choice of the domain hierarchy (3.1)*.*

Proof. The result can be derived by generalizing the proof of Theorem 3.5. This can be done by simply replacing $B^\ell_{M^\ell}$ by $D^\ell_{M^\ell}$ throughout the original proof. □

UCP should be quite useful when designing refinement algorithms that maintain the completeness property. Typically, the refinement is guided by an error estimator that selects the cells that need to be refined. Without UCP, further cells have to be added in order to maintain the completeness of the hierarchical space. This is no longer needed when using hierarchies with UCP and the decoupled hierarchical basis D of the spline space.

A sufficient condition for UCP is the following. For any choice of $\Omega^{\ell+1}$ and for any basis function $\beta \in B^\ell$ the support of any basis function $\gamma \in B^{\ell+1}$ with supp $\gamma \subseteq$ supp β intersects $\mathcal{M}^\ell$ in a connected set. Finally, we present two examples of hierarchies with UCP.

Example 4.5. UCP is satisfied when considering only single knots at all levels and using a refinement strategy that splits every cell of level ℓ in $p^\ell_1 \times \ldots \times p^\ell_d$ cells of level $\ell + 1$.

Example 4.6. When considering dyadic refinement, where every cell of level ℓ is split into 2^d cells of level $\ell + 1$, UCP is satisfied if the multiplicities are chosen such that the inequalities

$$3m^\ell_{i,j} \geq p^\ell_i + 1$$

hold for all levels, for $i = 1, \ldots, d$ and for $j \in \mathbb{Z}$.

Both examples include quadratic tensor-product splines with dyadic refinement. Special cases of both examples are shown in Figure 9. The B-splines β are decoupled into two basis functions $\delta_\Phi(\beta)$ and $\delta_\Psi(\beta)$ associated to the connected components $\Phi, \Psi \in CC(\Gamma_\beta)$. The finer subdomain is the region covered by the finer grid, whereas the coarser subdomain contains the entire mesh.

5. Closure

We analyzed dimensions and bases of multivariate tensor-product spline functions on a multi-cell domain. Based on these results, by a slight generalization of the techniques from [12], we derived a simple sufficient condition for the completeness of a hierarchical spline space. More precisely, this condition guarantees that any piecewise polynomial functions on the given hierarchical grid can be represented in the hierarchical tensor-product B-spline basis. In addition, we proposed the new concept of the *decoupled* hierarchical basis that allows to relax — and in the case of hierarchies with UCP even to eliminate — the conditions on the domain hierarchy that are required to guarantee the completeness.

Future work will focus on formulas for the dimensions of hierarchical spline spaces, which are currently only given implicitly by the number of active tensor-product B-splines, and on applications of multivariate hierarchical B-splines, in particular in isogeometric analysis.

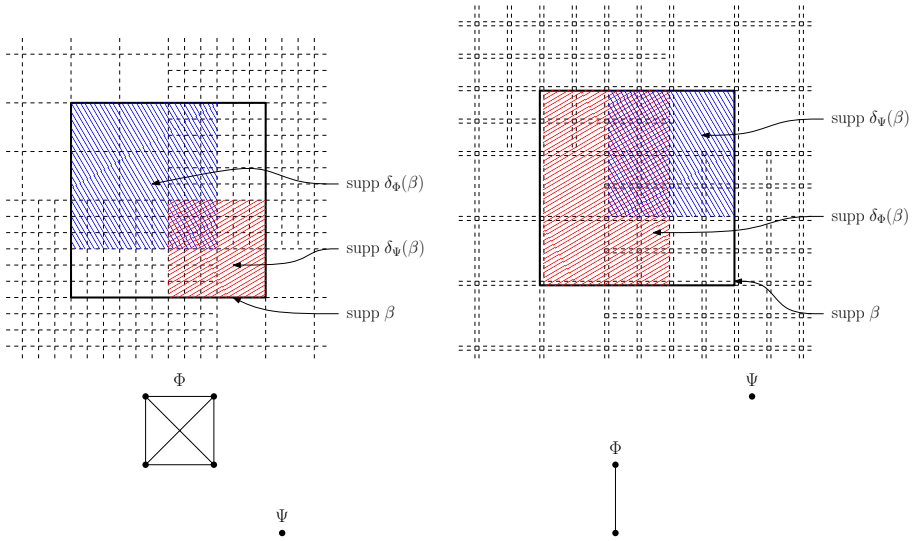

Figure 9: Two bivariate spline hierarchies with UCP. Top left: bicubic splines with single knots and triadic refinement. Top right: biquintic splines with double knots and dyadic refinement. Both pictures show the support of a B-spline β (solid black line) and of two decoupled basis functions $\delta_\Phi(\beta)$ and $\delta_\Psi(\beta)$ (red and blue regions) that are derived from the connected components Φ, Ψ of the coefficient graph of β. Bottom: the associated coefficient graphs.

Appendix A. The trivariate case with uniform knots and maximal smoothness

We consider Corollary 2.13 for spline spaces on multi-cell domains in three-dimensional space with maximal smoothness (i.e., all the multiplicities are equal to one). For simplicity, we consider uniform knots only, but all results remain valid in the non-uniform case. We derive formulas that give the number of B-splines, provided that the intersections of their supports with the multi-cell domains are connected. We show that the results by Berdinsky et al. [2] are a special case of this more general analysis.

Multi-cell domains and their properties have been studied in digital geometry [17]. However, most of the existing results are limited to simple polyhedra, i.e., multi-cell domains without kissing vertices and edge segments (see Subsection A.3 below), since these polyhedra are preferred in the relevant applications.

A.1. Dilations, offsets, and types of edges and vertices

Each of the basis functions of tri-degree $\mathbf{p} = (p, p, p)$, where p is a positive integer, can be identified with

- the centroid of the central cell of its support if p is even,
- the intersection of eight cells in the middle of the support if p is odd.

In order to derive the number of basis functions that have a support with a non-empty intersection with $\mathcal{M}$, we define the notion of *dilation* of a multi-cell domain. Moreover, we consider the so-called *combinatorial volume*, which is related to the number of cells and grid points of a multi-cell domain. The combinatorial volume of a multi-cell domain is then equal to the number of the basis functions of the spline space. Recall that the notion of a multi-cell domain refers both to a set M of cells and to the subset $\mathcal{M}$ of $\mathbb{R}^3$ that is occupied by them.

Definition A.1. The *dilation* $\mathcal{M}^{(q)}$ of a multi-cell domain $\mathcal{M}$, defined for any even value of q, is recursively obtained as

$$\mathcal{M}^{(q)} := \begin{cases} \mathcal{M}, & \text{if } q = 0, \\ \mathcal{M}^{(q-2)} \cup N(\mathcal{M}^{(q-2)}), & \text{for } q \geq 2, \end{cases}$$

where $N(\mathcal{M}^{(q-2)})$ is the *offset region of thickness* 1 *to* $\mathcal{M}^{(q-2)}$, i.e., the set of all the cells $c \in C$ that are contained in $\overline{\mathbb{R}^3 \setminus \mathcal{M}^{(q-2)}}$ and that share a vertex, an edge or a face with $\mathcal{M}^{(q-2)}$.

Clearly, the dilations of a multi-cell domain are again multi-cell domains. A related notion is the following.

Definition A.2. The *offset* of the multi-cell domain $\mathcal{M}$ at distance $q/2$ is the set

$$F^{(q)}(\mathcal{M}) := \left\{ \mathbf{x} \in \mathbb{R}^d \mid \inf_{\mathbf{r} \in \mathcal{M}} \max_{i=1,\ldots,d} (|r_i - x_i|) = \frac{q}{2} \right\}, \tag{A.1}$$

where $\mathbf{r} = (r_1, \ldots, r_d)$ is a point that belongs to the multi-cell domain $\mathcal{M}$. We assume $d = 3$.

The right-hand side of (A.1) is the set of points in Hausdorff distance $q/2$ (with respect to maximum metric) from $\mathcal{M}$. Geometrically, it is a generalization of the notion of the offset curve as defined in [12] to create a surface in three dimensions.

Note that the offset is defined for any nonnegative value of q, while the dilation is defined for even values only.

Dilations and offsets are closely related. For even values of q, the boundary of the dilation $\mathcal{M}^{(q)}$ is a subset of the offset $F^{(q)}(\mathcal{M})$. This characterization can be extended to odd values of q also, but we do not need it in this paper.

Definition A.3. The offset $F^{(q)}(\mathcal{M})$ is said to be *admissible*, or, equivalently, $\mathcal{M}$ is said to *admit an offset at distance* $\frac{q}{2}$, if either

- $q = 0$ holds or if
- $F^{(q-1)}(\mathcal{M})$ is admissible and all connected components of $F^{(q)}(\mathcal{M})$ are homeomorphic to a closed surface in $\mathbb{R}^3$ (i.e., to an embedded 2–manifold in 3–space).

Example A.4. The multi-cell domain shown in Figure A.10 admits an offset at distance $\frac{1}{2}$ but not at distance $\frac{2}{2} = 1$. Indeed, $F^{(2)}(\mathcal{M})$ is not homeomorphic to a closed surface.

Finally, we introduce another notion, which will be used to count the basis functions that are not identically zero on a multi-cell domain.

Definition A.5. The *q-th combinatorial volume* of a multi-cell domain $\mathcal{M}$ is defined as

$$\omega^{(q)}(\mathcal{M}) := \begin{cases} \text{number of cells of } \mathcal{M}^{(q)}, & \text{if } q \text{ is even;} \\ \text{number of grid points of } \mathcal{M}^{(q-1)}, & \text{if } q \text{ is odd.} \end{cases}$$

By *grid points* we mean the intersections of three grid hyperplanes.

A multi-cell domain can be characterized by various quantities. Its boundary consists of planar *patches* that consist of several *faces* (each belonging to only one cell). These patches meet in *edges* that consist of *edge segments* (each being incident to two or four faces). The edges meet in *vertices*. We consider

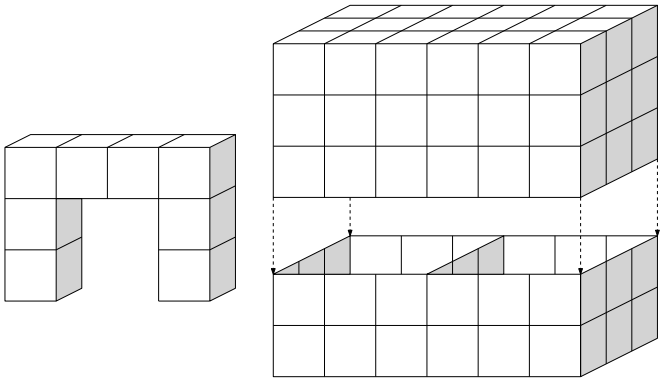

(a) domain (b) offset surface

Figure A.10: (a) Example of a multi-cell domain that is admissible for $q = 1$ but not for $q = 2$. (b) The non-admissible offset surface at distance 2.

- the number of cells z ,
- the number of boundary faces f,
- the number of convex edge segments e_{cvx}, of non-convex edge segments e_{ncx} and of kissing edge segments e_{ksg} (see Table A.1) on the boundary,

Table A.1: The types of boundary edges of a multi-cell domain.

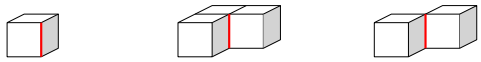

convex edge (cvx) | non-convex edge (ncx) | kissing edge (ksg)

- the number of vertices of type i, where $i = 1, \ldots, 21$ according to Table A.2, that will be denoted by v_i.

In addition, we use upper indices to denote the number of these quantities for the dilation $\mathcal{M}^{(q)}$. For instance, $z^{(q)}$, $e^{(q)}_{\text{cvx}}$ and $v^{(q)}_i$ denote the number of cells, convex edge segments, and vertices of type i of the dilation $\mathcal{M}^{(q)}$. Clearly, $z = z^{(0)}$ etc.

Finally, we introduce the *vertex term*

$$v^{(q)} = (v_1^{(q)} - 2v_3^{(q)} - 6v_4^{(q)} - 3v_5^{(q)} - v_6^{(q)} - v_7^{(q)} - 2v_9^{(q)} - 2v_{10}^{(q)} + 4v_{13}^{(q)} - v_{14}^{(q)} + v_{15}^{(q)} + 3v_{16}^{(q)} + 2v_{18}^{(q)} + 2v_{19}^{(q)} + v_{20}^{(q)}) \quad \text{(A.2)}$$

and the *edge term*

$$e^{(q)} = e^{(q)}_{\text{cvx}} - e^{(q)}_{\text{ncx}} - 2e^{(q)}_{\text{ksg}}. \quad \text{(A.3)}$$

Again, we shall omit the index $^{(q)}$ for $q = 0$, i.e., we write $v = v^{(0)}$, $e = e^{(0)}$ and $f = f^{(0)}$. Note that if $e_K = v_4 = v_{19} = 0$ (see Subsection A.3) then $v^{(q)}$ is equal to T from Theorem 8.6 in [17].

Table A.2: The types of vertices of a multi-cell domain, up to rotations and symmetries and ordered by the number of incident cells. The configurations marked by *, $^\circ$ and $^+$ do not correspond to vertices, since they are located within edges, within patches and in the interior of the multi-cell domain, respectively.

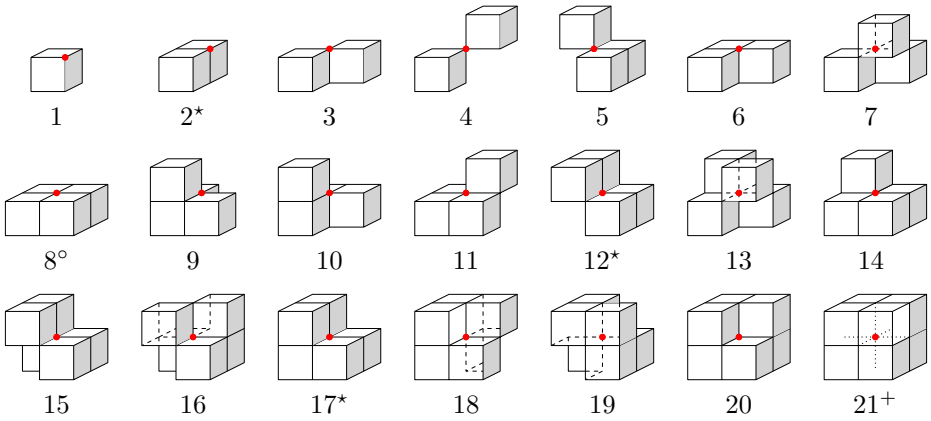

A.2. The dimension of the spline space

We derive the number of B-splines whose support intersects a given multi-cell domain and we specify it in terms of the quantities that characterise the domain $\mathcal{M}$. Lemma A.6 gives the formula for these quantities for the dilated domains $\mathcal{M}^{(q)}$ including the combinatorial volume $\omega^{(q)}(\mathcal{M})$ when q is even, while Lemma A.7 allows us to compute the combinatorial volume when q is odd. The dimension of the spline space is then described in Theorem A.8.

Lemma A.6. *If the multi-cell domain $\mathcal{M}$ admits an offset at distance $q/2$, where q is even, then the vertex term $v^{(q)}$, the edge term $e^{(q)}$, the number of faces $f^{(q)}$ and the number of cells $z^{(q)}$ of the dilated multi-cell domain $\mathcal{M}^{(q)}$ satisfy*

$$v^{(q)} = v,\ e^{(q)} = e + \frac{3q}{2}v,\ f^{(q)} = f + qe + \frac{3q^2}{4}v,\ z^{(q)} = z + \frac{q}{2}f + \frac{q^2}{4}e + \frac{q^3}{8}v. \tag{A.4}$$

Moreover, the formula for $z^{(q)}$ is valid even if $\mathcal{M}$ admits an offset at distance $\frac{q-1}{2}$ only.

Proof. Formulas (A.4) can be verified by induction (with respect to even values of q) using Table A.3. Given the dilation $\mathcal{M}^{(q)}$ of a multi-cell domain $\mathcal{M}$, the table specifies how the number of each kind of feature (i.e., faces, edge segments of the three types, and vertices of the 21 types) of the dilation $\mathcal{M}^{(q+2)}$ depends on the numbers of miscellaneous features in $\mathcal{M}^{(q)}$, provided that the offset at distance $(q+2)/2$ is admissible (except for the case of cells where we need only offset at distance $(q+1)/2$ to be admissible). This table can be derived by a careful case-by-case analysis. □

Lemma A.7. *The number of grid points $g(\mathcal{M})$ of a multi-cell domain $\mathcal{M}$ is equal to*

$$g(\mathcal{M}) = z + \frac{f}{2} + \frac{e}{4} + \frac{v}{8}.$$

Lemma A.7 can be proved by inspecting various cases similarly to Lemma A.6.

Based on the previous two lemmas and on Corollary 2.13, we are now able to formulate the main result of this appendix.

Table A.3: Numbers of cells, faces, convex/non-convex/kissing edge segments and vertices of the various types of the dilation $\mathcal{M}^{(q+2)}$ that are contributed by each cell, face, edge segment and vertex of $\mathcal{M}^{(q)}$. The proof of Lemma A.6 is based on this information.

			dilation $\mathcal{M}^{(q+2)}$																				
			cell	face	edge			vertex															
					cvx	ncx	ksg	1	3	4	5	6	7	9	10	11	13	14	15	16	18	19	20
multi-cell domain $\mathcal{M}^{(q)}$	cell		1																				
	face		1	1																			
	edge	cvx	2	2	1																		
		ncx	-2	-2		1																	
		ksg	-4	-4		2																	
	vertex	1	1	3	3			1															
		3	-2	-6	-4	2						2											
		4	-6	-18	-6	12												6					
		5	-3	-9	-3	6												3					
		6	-1	-3	-2	1						1											
		7	-1	-3	-3									1									1
		9	-2	-6	-3	3								1									
		10	-2	-6	-2	4												2					
		11			-1	-1												1					1
		13	4	12		-12																	4
		14	-1	-3	-1	2												1					
		15	1	3		-3																	1
		16	3	9		-9																	3
		18	2	6		-6																	2
		19	2	6		-6																	2
		20	1	3		-3																	1

Theorem A.8. *Consider a multi-cell domain $\mathcal{M}$ that admits an offset at distance $(p-1)/2$, where p is a non-negative integer. Then the p–th combinatorial volume of $\mathcal{M}$ — and therefore also the dimension of $\mathbb{S}(M)$ — is equal to*

$$\omega^{(p)}(\mathcal{M}) = z + \frac{p}{2}f + \frac{p^2}{4}e + \frac{p^3}{8}v, \tag{A.5}$$

where z and f are the number of cells and boundary faces, respectively, while the vertex and edge terms $v = v^0$ and $e = e^0$ have been defined in equations (A.2) *and* (A.3)*.*

Proof. For even values of p we have that

$$\omega^{(p)}(\mathcal{M}) = z^{(p)}$$

and thus (A.5) follows from Lemma A.6.

For odd values of p, we obtain $\omega^{(p)}(\mathcal{M}) = g(\mathcal{M}^{(p-1)})$. Using Lemma A.7, we obtain

$$g(\mathcal{M}^{(p-1)}) = z^{(p-1)} + \frac{1}{2}f^{(p-1)} + \frac{1}{4}e^{(p-1)} + \frac{1}{8}v^{(p-1)}. \tag{A.6}$$

Using Lemma A.6, equation (A.6) implies (A.5). This is where we need the assumption regarding the admissibility of the offset at distance $\frac{p-1}{2}$.

According to Corollary 2.13, the combinatorial volume is equal to the dimension of $\mathbb{S}(M)$, since the combinatorial volume is equal to the cardinality of B_M and the admissibility of the

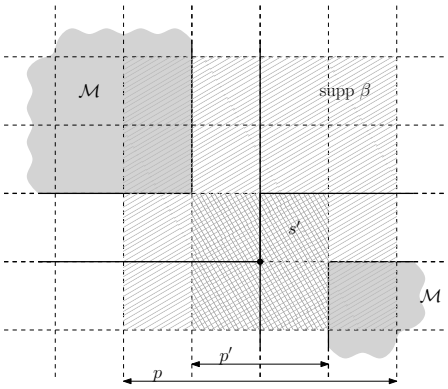

Figure A.11: If the coefficient graph of a basis function β has two connected components, then shrinking supp β (single hatching) gives a cube s' (double hatching) that touches the boundary of $\mathcal{M}$ (solid light gray) in at least two disjoint sets of points. The center of s' (black dot) belongs to a self–intersetion of a certain offset (thick solid black line).

offset implies the assumption of that Corollary[2]. Indeed, if there is a basis function whose coefficient graph has at least two connected components, then we may "shrink" its support to a cube s' constisting of $p' \times p' \times p'$ times cells, where $p' \leq p-1$ is as small as possible, and so that this cube still "touches" cells from two components (that is, it contains two points from two different components but $(s')^\circ \cap \mathcal{M}^\circ = \emptyset$, see Figure A.11 for a bivariate analogy). The center of s' belongs a self-intersection of the offset at distance $\frac{p'}{2}$ and thus the offset at distance $\frac{p-1}{2}$ is not admissible. □

A.3. The case of topological manifolds with boundaries

The remainder of this appendix relates our result to the dimension formula of Berdinsky et al. [2, Corollary 8]. Note that this paper also derives other dimension formulas that do not rely on the admissibility of offsets but on other topological constraints [2, Corollary 7].

Lemma A.9. *For any multi-cell domain $\mathcal{M}$ we have that*

$$\begin{aligned} c + f\frac{p}{2} + (e_{\text{cvx}} - e_{\text{ncx}} - 2e_{\text{ksg}})\frac{p^2}{4} + v\frac{p^3}{8} = \\ = c(p+1)^3 - f_{\text{itl}}\, p(p+1)^2 + (e_{\text{itl}} - e_{\text{ksg}})p^2(p+1) + \\ + (-v_4 + v_7 + v_{11} + v_{12} + 3v_{13} + v_{15} + 2v_{16} + v_{18} + v_{19} - v_{21})p^3. \end{aligned} \quad \text{(A.7)}$$

where f_{itl} and e_{itl} are the number of internal faces and internal edges (faces and edges of cells that are contained in the interior of $\mathcal{M}$), respectively.

Proof. We compare the coefficients of the powers of p on both sides of the equation.

p^0: We have $c = c$.

p^1: We need to prove that

$$6c = 2f_{\text{itl}} + f. \quad \text{(A.8)}$$

[2]Clearly, the admissibility of the offsets is sufficient but not necessary for this assumption to be satisfied; consider, e.g., uniform triquadratic splines on $3 \times 3 \times 3$ cells with the central cell removed.

This equation is satisfied since each cell has six faces and all internal faces belong to two cells.

p^2: We need to prove that

$$3c - 2f_{\mathrm{itl}} + e_{\mathrm{itl}} - e_{\mathrm{ksg}} = \frac{1}{4}(e_{\mathrm{cvx}} - e_{\mathrm{ncx}} - 2e_{\mathrm{ksg}}). \tag{A.9}$$

Consider the two identities

$$\begin{aligned} 4f &= 2e_{\mathrm{cvx}} + 2e_{\mathrm{ncx}} + 4e_{\mathrm{ksg}} + 2e_{\mathrm{flt}} \\ 4f_{\mathrm{itl}} &= 2e_{\mathrm{ncx}} + 4e_{\mathrm{itl}} + e_{\mathrm{flt}}. \end{aligned}$$

where e_{flt} is the number of flat edges, i.e., edges within patches of the boundary of the multi-cell domain (shared by two co-planar boundary faces). These two identities imply

$$-4f_{\mathrm{itl}} + 2f + 4e_{\mathrm{itl}} - 4e_{\mathrm{ksg}} = e_{\mathrm{cvx}} - e_{\mathrm{ncx}} - 2e_{\mathrm{ksg}}.$$

Dividing by four and using again (A.8) leads to (A.9).

p^3: We need to prove that

$$\begin{aligned} &8(c - f_{\mathrm{itl}} + e_{\mathrm{itl}} - e_{\mathrm{ksg}} + (-v_4 + v_7 + v_{11} + v_{12} + 3v_{13} + v_{15} + 2v_{16} + v_{18} + v_{19} - v_{21})) = \\ &\quad = (v_1 - 2v_3 - 6v_4 - 3v_5 - v_6 - v_7 - 2v_9 - 2v_{10} + 4v_{13} - v_{14} + v_{15} + 3v_{16} + 2v_{18} + 2v_{19} + v_{20}). \end{aligned} \tag{A.10}$$

Each cell has eight vertices, thus

$$\begin{aligned} 8c &= v_1 + 2v_2 + 2v_3 + 2v_4 + 3v_5 + 3v_6 + 3v_7 + 4v_8 + 4v_9 \\ &\quad + 4v_{10} + 4v_{11} + 4v_{12} + 4v_{13} + 5v_{14} + 5v_{15} + 5v_{16} + 6v_{17} + 6v_{18} + 6v_{19} + 7v_{20} + 8v_{21}. \end{aligned} \tag{A.11}$$

Similarly, each face has four vertices, hence

$$\begin{aligned} 4f_{\mathrm{itl}} = v_2 + v_5 + 2v_6 + 4v_8 + 3v_9 + 3v_{10} + 2v_{11} + 2v_{12} + 5v_{14} + 4v_{15} + 3v_{16} \\ + 7v_{17} + 6v_{18} + 6v_{19} + 9v_{20} + 12v_{21}. \end{aligned}$$

Moreover, each edge has two vertices, thus

$$2e_{\mathrm{itl}} = v_8 + v_{14} + 2v_{17} + v_{18} + 3v_{20} + 6v_{21} \tag{A.12}$$

and

$$2e_{\mathrm{ksg}} = v_3 + v_5 + 3v_7 + 2v_{11} + 2v_{12} + 6v_{13} + v_{15} + 3v_{16} + v_{18}. \tag{A.13}$$

A suitable linear combination of (A.11)–(A.13) gives (A.10). □

Corollary A.10. *Consider a multi-cell domain $\mathcal{M}$ with $e_{\mathrm{ksg}} = 0$, $v_4 = 0$ and $v_{19} = 0$ that admits an offset at distance $\frac{p-1}{2}$. Then*

$$\begin{aligned} \mathcal{V}^{(p)}(\mathcal{M}) &= c + f\frac{p}{2} + (e_{\mathrm{cvx}} - e_{\mathrm{ncx}})\frac{p^2}{4} + (v_1 - v_6 - 2v_9 - 2v_{10} - v_{14} + v_{20}) = \\ &= c(p+1)^3 - f_{\mathrm{itl}}p(p+1)^2 + e_{\mathrm{itl}}p^2(p+1) - v_{21}p^3. \end{aligned} \tag{A.14}$$

Proof. Since $e_{\mathrm{ksg}} = 0$, there are no vertices that are incident to a kissing edge, i.e.,

$$v_3 = v_5 = v_7 = v_{11} = v_{12} = v_{13} = v_{15} = v_{16} = v_{18} = 0.$$

Substituting these values into (A.7) gives (A.14). □

Equation (A.14) shows that the result of [2, Corollary 8] is a special case of Theorem A.8. Note that a multi-cell domain with $e_{\mathrm{ksg}} = v_4 = v_{19} = 0$ is called a topological manifold with boundary in [2].

Acknowledgements

The authors have been supported by the Austrian Science Fund (FWF), NFN S117 "Geometry + Simulation" and by the EC, project EXAMPLE, GA No. 324340. This support is gratefully acknowledged.

References

[1] Y. Bazilevs, V. M. Calo, J. A. Cottrell, J. Evans, T. J. R. Hughes, S. Lipton, M. A. Scott, and T. W. Sederberg. Isogeometric analysis using T-Splines. *Comput. Methods Appl. Mech. Engrg.*, 199:229–263, 2010.

[2] D. Berdinsky, T. Kim, C. Bracco, D. Cho, B. Mourrain, M. Oh, and S. Kiatpanichgij. Dimensions and bases of hierarchical tensor-product splines. *J. Comput. Appl. Math.*, 257:86–104, 2014.

[3] D. Berdinsky, T. Kim, C. Bracco, D. Cho, M. Oh, and Y. Seo. Iterative refinement of hierarchical T-meshes for bases of spline spaces with highest order smoothness. *Comput. Aided Design*, 47:96–107, 2014.

[4] D. Berdinsky, T. Kim, D. Cho, and C. Bracco. Bases of T-meshes and the refinement of hierarchical B-splines. https://sites.google.com/site/berdinsky/.

[5] P. B. Bornemann and F. Cirak. A subdivision-based implementation of the hierarchical B-spline finite element method. *Comput. Methods Appl. Mech. Engrg.*, 253:584–598, 2013.

[6] J. A. Cottrell, T. J. R. Hughes, and Y. Bazilevs. *Isogeometric Analysis: Toward Integration of CAD and FEA*. John Wiley & Sons, 2009.

[7] J. Deng, F. Chen, and Y. Feng. Dimensions of spline spaces over T–meshes. *J. Comput. Appl. Math.*, 194:267–283, 2006.

[8] J. Deng, F. Chen, X. Li, Ch. Hu, W. Tong, Z. Yang, and Y. Feng. Polynomial splines over hierarchical T-meshes. *Graph. Models*, 70:76–86, 2008.

[9] T. Dokken, T. Lyche, and K. F. Pettersen. Polynomial splines over locally refined box–partitions. *Comput. Aided Geom. Design*, 30:331–356, 2013.

[10] M. R. Dörfel, B. Jüttler, and B. Simeon. Adaptive isogeometric analysis by local h-refinement with T-splines. *Comput. Methods Appl. Mech. Engrg.*, 199:264–275, 2010.

[11] D. R. Forsey and R. H. Bartels. Hierarchical B-spline refinement. *Comput. Graphics*, 22:205–212, 1988.

[12] C. Giannelli and B. Jüttler. Bases and dimensions of bivariate hierarchical tensor–product splines. *J. Comput. Appl. Math.*, 239:162–178, 2013.

[13] C. Giannelli, B. Jüttler, and H. Speleers. THB–splines: the truncated basis for hierarchical splines. *Comput. Aided Geom. Design*, 29:485–498, 2012.

[14] C. Giannelli, B. Jüttler, and H. Speleers. Strongly stable bases for adaptively refined multilevel spline spaces. *Adv. Comput. Math.*, 2014. To appear.

[15] G. Greiner and K. Hormann. Interpolating and approximating scattered 3D-data with hierarchical tensor product B-splines. In A. Le Méhauté, C. Rabut, and L. L. Schumaker, editors, *Surface Fitting and Multiresolution Methods*, Innovations in Applied Mathematics, pages 163–172. Vanderbilt University Press, Nashville, TN, 1997.

[16] G. Kiss, C. Giannelli, and B. Jüttler. Algorithms and data structures for truncated hierarchical B-splines. In M. Floater et al., editors, *Mathematical Methods for Curves and Surfaces*, volume 8177 of *Lecture Notes in Computer Science*, pages 304–323. Springer, 2014.

[17] R. Klette and A. Rosenfeld. *Digital Geometry: Geometric Methods for Digital Picture Analysis*. Morgan Kaufmann, 2004.

[18] R. Kraft. Adaptive and linearly independent multilevel B–splines. In A. Le Méhauté, C. Rabut, and L. L. Schumaker, editors, *Surface Fitting and Multiresolution Methods*, pages 209–218. Vanderbilt University Press, Nashville, 1997.

[19] G. Kuru, C. V. Verhoosel, K. G. van der Zeeb, and E. H. van Brummelen. Goal-adaptive isogeometric analysis with hierarchical splines. *Comput. Methods Appl. Mech. Engrg.*, 270:270–292, 2014.

[20] X. Li, J. Deng, and F. Chen. Dimensions of spline spaces over 3D hierarchical T-meshes. *J. of Information & Computational Science*, 3:487–501, 2006.

[21] X. Li, J. Deng, and F. Chen. Surface modeling with polynomial splines over hierarchical T-meshes. *Visual Comput.*, 23:1027–1033, 2007.

[22] X. Li, J. Deng, and F. Chen. Polynomial splines over general T-meshes. *Visual Comput.*, 26:277–286, 2010.

[23] B. Mourrain. On the dimension of spline spaces on planar T–meshes. *Math. Comp.*, 83:847–871, 2014.

[24] K. F. Pettersen. On the dimension of multivariate spline spaces. *Report SINTEF A23875*, 2013.

[25] H. Prautzsch, W. Boehm, and M. Paluszny. *Bézier and B–spline Techniques*. Springer, 2002.

[26] D. Schillinger, L. Dedé, M. A. Scott, J. A. Evans, M. J. Borden, E. Rank, and T. J. R. Hughes. An isogeometric design-through-analysis methodology based on adaptive hierarchical refinement of NURBS, immersed boundary methods, and T-spline CAD surfaces. *Comput. Methods Appl. Mech. Engrg.*, 249:116 – 150, 2012.

[27] L. L. Schumaker and L. Wang. Approximation power of polynomial splines on T–meshes. *Comput. Aided Geom. Design*, 29:599–612, 2012.

[28] T. W. Sederberg, J. Zheng, A. Bakenov, and A. Nasri. T-splines and T-NURCCS. *ACM Trans. Graphics*, 22:477–484, 2003.

[29] A.-V. Vuong, C. Giannelli, B. Jüttler, and B. Simeon. A hierarchical approach to adaptive local refinement in isogeometric analysis. *Comput. Methods Appl. Mech. Engrg.*, 200:3554–3567, 2011.